Adiposity QTL *Adip20* decomposes into at least four loci when dissected using congenic strains

Cailu Lin, Brad D. Fesi, Michael Marquis, Natalia P. Bosak, Anna Lysenko, Mohammed Amin Koshnevisan, Fujiko F. Duke, Maria L. Theodorides, Theodore M. Nelson, Amanda H. McDaniel, Mauricio Avigdor, Charles J. Arayata, Lauren Shaw, Alexander A. Bachmanov and Danielle R. Reed

Monell Chemical Senses Center, 3500 Market St, Philadelphia PA

Please address correspondence:
Danielle R. Reed, Ph.D.
Monell Chemical Senses Center
3500 Market St
Philadelphia PA 19104
reed@monell.org

Abstract

An average mouse in midlife weighs between 25 and 30 g with about a gram of tissue in the largest adipose depot (gonadal) but the weight of this depot differs among inbred strains. As an example, we found that mice from the C57BL/6ByJ strain have heavier gonadal depots than did 129P3/J mice. To understand the genetic contributions to this trait, we mapped several quantitative trait loci (QTLs) for gonadal depot weight in an F_2 intercross population. Our goal here was to fine map one of these QTLs, *Adip20* (formerly *Adip5*) on mouse chromosome 9. To that end, we analyzed the weight of the gonadal adipose depot from mice from newly created congenic strains. Using the sequential comparison method, the results indicated at least four rather than one QTL; two of the QTL were less than 0.5 Mb apart with opposing directions of allelic effect. Different types of evidence (missense genetic variation, human adiposity/body mass index orthologues and differential gene expression) implicated numerous candidate genes from the four QTL regions. These results highlight the value of mouse congenic strains and the sequential method to dissect challenging genetic architecture.

An average mouse at six months of age weighs about 25 to 30 g. Some of this weight is due to adipose tissue located in several depots, the largest of which is the gonadal (**Figure 1**). In rodents, depots can differ in weight up to 20-fold, depending on the particular strain, and while adipose depot weight is highly heritable [1, 2], there are specific genetic determinants for each depot which reflect its specialized functions[3]. Investigators have interbred specific strains and looked for chromosomal regions that affect the weight of individual adipose depots and this procedure has identified hundreds of influential genomic regions, or quantitative trait loci (QTLs), which curators catalog in the Mouse Genome Database [4]. While it has been difficult to identify the underlying genetic variants for many complex traits including adiposity [5], it remains an important scientific goal because of its potential of this knowledge to better explain genetic risks and suggest new biological pathways and therapeutic targets [6].

Our specific goal here was to map loci for gonadal adipose depot weight in mice and identify the underlying genetic variants using a pair of contrasting inbred strains. We began QTL mapping by intercrossing the C57BL/6ByJ (B6) strain with the 129P3/J (129) strain [7-9] and found a QTL on chromosome 9, which we originally called *Adip5* (at ~50 Mb) but which was renamed *Adip20*. Chromosomal mapping using intercross populations did not provide sufficient resolution to narrow the genomic interval to specific candidate genes, so our next step was to refine the location of this QTL by creating and studying mouse congenic strains. We assayed or imputed genotypes for a common set of markers on mouse chromosome 9 and analyzed the genotype-phenotype associations using several computational approaches including a sequential method of strain comparison [10]. Maternal effects and imprinting affect body composition so we incorporated several experimental design features to control these influences. After the mapping studies, we used several methods to identify candidate genes (DNA sequencing, human homology and microarray studies).

Method

Animal husbandry. We bred all mice in the animal vivarium at the Monell Chemical Senses Center, located in Philadelphia, Pennsylvania (USA), except for the inbred B6 and 129 mice used for the first stages of breeding, purchased from the Jackson Laboratory. During this time, husbandry practices were stable, owing in part to having the same vivarium personnel and in part to using a consistent type of bedding (Aspen Shavings, Northeastern Products Corp, Warrensburg, NY). We fed mice Rodent Diet 8604 (Harlan Teklad, Madison, WI) and they lived in a 12:12 light cycle, with lights off at 6 pm, barring unusual circumstances (e.g., weather-related power outages). The Monell Institutional Animal Care and Use Committee approved these procedures.

We started branching congenic mice by backcrossing N_6 (F_1 x B6) males (from heterozygous consomic B6.129-Chr9 mice[11] with partial donor chromosome 9) to the B6 females to produce mice with 129-derived donor chromosomal regions of various lengths. We named the strains with codes that reflect their lineage; for instance, all strains with the prefix 1 (e.g., 1.1) descended from common progenitors. The breeding goal was to identify male breeders possessing a donor region that overlapped the QTL location discovered in the original F_2 intercross.

We bred congenic mice that had either zero or one copies of the 129-derived donor region by mating inbred B6 female mice with heterozygous congenic males. This approach reduced maternal effects (all mothers were the same genotype), and reduced imprinting effects (only fathers contributed the donor region). Each congenic mouse was potentially genetically unique (because the paternal donor region could shorten due to meiotic recombination). Therefore, we genotyped each congenic mouse to ensure we could define the donor region breakpoints. While most mice had full-length donor regions, some had shorter regions we refer to as 'partial'.

Genotyping. We evaluated simple sequence-length polymorphism markers (e.g., *D9Mit2*) by polyacrylamide gel electrophoresis after polymerase chain reaction amplification by locus-specific primers [12] in our laboratories. We assayed single nucleotide polymorphisms (SNPs) in three locations: at the Genotyping and RNA Analysis Core at the Monell Chemical Senses Center; at the Center for Inherited Disease Research (see Electronic Resources) as part of an NIH-funded genotyping supplement; or by a commercial vendor (LGC, Beverly, MA; formerly KBiosciences) as a fee-for-service. When assaying variants in the Monell genotyping core, we used primers and allele-specific dye-labeled probes (Life Technologies, Carlsbad, CA). Irrespective of genotype location, controls (blank samples, and genomic DNA from inbred progenitors and their F_1 hybrids) were included in genotyping with all assays, and we retested unlikely genotypes as needed. We list all markers tested and their base pair positions relative to GRCm38 in **Supplemental Table 1.** We imputed missing data by tracing the parental origin of the marker alleles and assuming that no double recombination occurred between markers 26 Mb or less apart. We selected this 26 Mb criterion as the smallest distance between two observed recombinant events in the most densely genotyped populations we have studied [11]. We also genotyped 12 representative congenic mice to evaluate residual genetic background using the Mouse Universal Genotyping Array (www.neogen.com) with 7,851 SNP markers built on the Illumina platform. We tallied the numbers of heterozygous markers in the genetic background (excluding the targeted donor regions) and expressed them as a fraction of the total valid markers for an estimate of residual heterozygosity.

Phenotyping measures. After euthanasia by carbon dioxide affixation, we weighed the body of each mouse to the nearest 0.1 g. During necropsy, we removed the gonadal adipose depot using anatomic landmarks [13, 14] and weighed the wet tissue to the nearest 0.1 g.

Gonadal adipose depot gene expression. We conducted two microarray experiments to quantify gonadal depot adipose tissue gene expression between congenic mice with and

without the donor region (Experiment 1 and 2). In Experiment 1, we selected tissue from male mice from congenic strain 4. We chose this strain because the donor region captured the *Adip20* peak we previously identified [15] (42.6 to 58.3 Mb). Half of the mice were heterozygous for the donor region (129/B6; N=7) and half were littermates homozygous for the donor region (B6/B6; N=7). Experiment 2 was a replication except there were six mice in each genotype group for a total of 12 mice. We isolated RNA from each gonadal adipose depot and measured genome-wide exon-by-exon expression using the Affymetrix Mouse Gene 1.0 ST Array. Members of the University of Pennsylvania Microarray Core facility, prepared the RNA, performed the chip hybridization and did preliminary quality control steps following the manufacturer directions.

Data analysis. We took three steps to prepare for the statistical analysis of the gonadal adipose depot weights. First, we eliminated data from mice that (a) appeared to be sick (e.g., hunched posture) or (b) had tumors or other obvious gross morphology found during necropsy (**Supplemental Table 2**). Next, we determined whether the data were normally distributed using the *fitdistrplus* R package [16], log-transformed the data (**Supplemental Figure 1)** if needed, and confirmed this transformation was effective using the Kolmogorov-Smirnov (K-S) test (**Supplemental Table 3).** Finally, we evaluated the importance of body weight and age as covariates using Pearson correlation coefficients. We observed that body weight was highly correlated with adipose depot weight (**Supplemental Figure 2A**) but age, owing to the tight range, measured in days, was not (**Supplemental Figure 2B).** Therefore, we used body weight but not age as a covariate for all subsequent analyses.

To reveal the specific QTL locations, we analyzed the congenic data using several approaches. In the first approach, we treated all congenic mice as though they were from the same mapping population, and conducted a general linear model analysis of the log transformed gonadal adipose depot weight for each marker, using marker genotype as a fixed

factor and body weight as a covariate, and using a type 1 (sequential) sum of squares. For the presentation of the data, we (a) computed marker association test statistics and converted the associated p-values to the negative logarithm with base 10, (b) calculated the genotype mean, and (c) calculated the effect sizes using Cohen's *D* [17] for the peak linked marker in each mapping population. We defined a 'significant' statistical threshold as an α level of 0.05 after Bonferroni correction for the number of markers (N=148; $-log10\frac{\alpha}{N}$= 3.47) and a suggestive threshold as an α level of 0.63 ($-log10\frac{\alpha}{N}$= 2.37) [18].

Next, we analyzed congenic data using sequential method that can detect single and multiple QTL [19]. The sequential method compares congenic strains in a predetermined order. To establish the appropriate order for this strain comparison, a minimum spanning tree of the congenic strains (N=12 strains; all group sizes ≥ 12) , we wrote a custom R-script following the previously published pseudocode ([19] supplemented with the R software package *optrees* [20] and *igraph* [21]). The original version of the sequential analysis compares an inbred host strain and multiple homozygous congenic strains. Instead, here we compared heterozygous congenic mice (129/B6) to their homozygous littermates (B6/B6). To make these comparisons, we used a general linear model followed by least-squares difference post hoc analysis. We also analyzed the congenic data with the classic 'common segment' method that is best suited for the detection of single QTL in two ways, incorporating only the strains with the largest group sizes (narrow) and then nearly all congenic strains (broad).

DNA sequence variants and human homology. Using an online database [22], we identified all genes residing within the genomic coordinates of the QTLs defined in the sequential congenic analysis. We next used another online database [23] containing genomic variants among inbred mouse strains from a large-scale genome sequencing project [24, 25] to compare the genomic sequences within the defined QTL regions for strains (129P2/OlaHsd and

C57BL/6J) closely related to parental inbred strains used in our study. We identified sequence (missense and stop codon gain/loss) with the potential to cause functional changes. We determined which variants were likely to be functional using computer algorithms in the program Sorting Intolerant From Tolerant [26]. Eight SNPs were excluded from this analysis because we could find no unique identifier for the variant in the dbSNP database (Build 138) [27]. We also identified human genes and their variants associated with obesity that are located in the regions of conserved synteny with the mouse QTL regions by searching an online catalog of human genome-wide association results [28] with key words “adipose” and “body mass index”.

Analysis of microarray data. We performed gene expression analysis using Partek® Genomics Suite® (version 6.6, build 6.16.0419) by importing CEL files of raw intensities for each probe set, performing the post-import quality control analyses and compared genotype groups (host versus donor region) for differential gene expression [29-31]. We report the differential expression as the log2 fold-change with an associated p-values corrected for false discovery for the number of genes examined [32]. We filtered the relevant genes using a customized volcano plot (e.g., [33]) using criterion of absolute $\log_2$FoldChange≥1 and FDR <0.05 with the text labeled in *maptools* R package [34]. We compared the results between Experiment 1 and Experiment 2 and report only those genes which differed consistently (absolute $\log_2$FoldChange ≥1 or FDR p-value <0.05) by genotype in both studies. We report differentially expressed candidate genes within the entire congenic donor region reasoning that gene regulatory elements can be located over millions of base pairs from their protein coding regions [35].

For all analyses listed above except of the gene expression data, we computed the statistical tests with R (version 3.2.0) and R-studio (version 0.99.489) and graphed the results using GraphPad Prism 6 (version 6.05; GraphPad Software, La Jolla, CA). All data are available for download on Github (https://github.com/DanielleReed/Adip20) and the Center for Open

Science (osf.io/yeqjf) [36]. All mouse physical map locations are in base pairs using GRCm38 (mm10).

Results

Dissection of adiposity loci. We studied 1,293 congenic mice in total from 22 strains (**Table 1, Supplemental Table 4**) and confirmed the residual level of residual heterozygosity of these newly created strains was low (>0.2%). In an initial analysis of a combined group of mice from all congenic strains, we estimated effect of marker genotype on gonadal adipose depot weight using the general linear model (**Figure 2**). These results confirmed a linkage with the large effect size at ~52.5 Mb but also indicated other peaks (**Figure 2A**).

Therefore using the sequential method, analyzed the congenic strains with group sizes N ≥ 12 (**Supplemental Table 5**). We put the 12 congenic strains which met this group-size criterion into one of three groups for comparison; the groupings and comparison order (described below) was suggested by the results of the minimum spanning tree (MST) analysis (**Figure 3A)**. Within these groups, we compared pairs of strains, in a predetermined order, starting from comparison of the host strain (littermates without the donor fragment) and the strain with the smallest donor region (**Figure 3B)**. The sequential analysis results indicated the presence of four QTLs (**Figure 3C**) and we ordered these QTL from proximal to distal, starting with QTL 1. For QTLs 1, 2, and 4, the 129-derived allele increased the weight of the gonadal adipose depot, whereas QTL3 had the opposite direction of effect. As expected, the common segment method was uninformative for both the narrower and broader analysis, failing to point to one region with a single QTL (see **Supplemental Text 1; Supplemental Tables 4-8**).

Genetic variations. We analyzed genes residing in the QTL regions estimated in the sequential congenic analysis: QTL1, 9:42779420-44142555; QTL2, 9:48789608-53884418; QTL3, 9:54242579-54286770; and QTL4, 9:58262383-124595110. We refined the poorly

localized QTL4 drawing on marginally significant mapping results from the F_2 [15] to marker *rs3721068* with a 10 Mb flanking region (QTL4, 9:108915010-118915010). Within these genomic coordinates for the four QTL, there are 429 protein-coding genes [22]. Forty-eight of these genes have sequence variants between the 129P2/OlaHsd and C57BL/6J strains (closely related to the B6 and 129 parent strains used in our study), which were either missense or (for two genes, *1110032A03Rik* and *Camp*) predicted gain/loss variants of stop codons (see **Supplemental Table 9**). Many insertions/deletions of unknown significance are also in these regions. Using these QTL co-ordinates, we surveyed the mouse genome database [4] for other adiposity QTLs on chromosome 9. Of the eight previously reported QTLs (*Adip5*, *Adip14*, *Dob2*, *Mobq8*, *Obq5*, *Carfhg2*, *Plbcq5* and *Tdmq1*), seven QTL had overlapping confidence intervals with the QTLs reported here (**Supplemental Table 10**).

Human orthologues. Using the genomic coordinates given above, we identified the regions of conserved synteny of the human chromosomes 3, 11 and 15. We next examined results of recent human genome-wide association studies to find genes associated with body mass index and adiposity [28] and residing in these regions (**Table 2**), and to examine if their mouse orthologous genes with sequence variants. Four human genes (*FDX1*, *ARHGAP20*, *PDCD6IP,* and *TRAK)* associated with adiposity and six (*C11orf53*, *NCAM1*, *DMXL2*, *OSBPL10*, *LOC101928114,* and *CCK*) associated with body mass index (a commonly used but indirect measure of human adiposity) resided in these regions. Among mouse orthologs of these ten genes, at least one, *Osbpl10*, has a protein-coding variant between 129P2/OlaHsd and C57BL/6J strains closely related to the B6 and 129 parental strains used in our study.

Microarray results. Eleven genes (*Dixdc1, Cryab, Sik2, Sik3, Isl2, Arcn1, Fam55d, hmbs, Il10ra, Fxyd6, Mcam*) within the donor region of the congenic strain 4 (42.6 to 58.3 Mb; **Figure 3C**) were consistently differentially expressed in the gonadal adipose tissue of mice with different genotypes (**Figure 4**, and **Supplemental Table 11)**. Of the differentially expressed

genes, *Dixdc1* and *Sik2* had two missense mutations for each between the related parental strains (**Supplemental Table 9).** We compared the results from the three methods to evaluate candidate genes (parental sequence differences, human orthologues and differential gene expression) and but there was no convergence to particular candidate genes (**Figure 5**).

Discussion

Here we bred congenic strains with the expectation that we could narrow the genomic location of an adiposity QTL, *Adip20*, to a region with only one or a very few genes on mouse chromosome 9. The successful identification of several obesity genes including leptin [37], the leptin receptor [38], tubby [39, 40], and agouti [41] suggested this strategy would be useful even when effect sizes differ by genetic context [42]. These early successes spawned other efforts like ours to map genetic variants that contribute to obesity [43-60] and investigators have identified hundreds of QTLs [4]. When we fine-mapped the *Adip20* locus, we detected effects of at least four QTL on chromosome 9. These results illustrate both the complexity of body composition genetics, and the utility of congenic strains to better characterize the underlying genetic architecture and further suggest that decomposition of a single QTL into multiple QTL is commonplace for traits like adipose depot weight and obesity [61, 62].

In general, the study of complex traits is easier when we reduce or eliminate extraneous sources of trait variation. For obesity, sex by genotype interactions are a common feature of natural populations, including humans [63] and are often detected in mouse intercross studies [8, 64, 65]. Thus, we chose to study only male mice to reduce the potential interaction of a particular genotype with sex while acknowledging this choice makes the results less generalizable [66]. We cannot quantify the choice was effective but it did contribute generally to the statistical power of the analysis by reducing sex-specific variation. However, an important limitation of this study is that is applies to males only, and the results for female mice could be very different.

In addition to reducing variation in adiposity due to sex, we controlled age as a source of potential trait variation to reduce genotype by age interactions [67]. We also tried to reduce parent-of-origin and maternal effects because of their known influence on adiposity [68, 69]. We controlled some maternal effects in the sense that all congenic mice had mothers of the same genotype and we controlled some imprinting and other parent of origin effects because all congenic mice inherited the donor region from the father (i.e., paternal transmission). We acknowledge that maternal effects are a composite of many factors, not only maternal genotype and so the offspring may vary based on maternal body weight and parenting behavior. However, generally, these experimental choices were useful in reducing certain types of variation but studying only mice of a single sex, the exact benefit to power and genetic mapping accuracy is difficult to evaluate quantitatively.

Obesity as a trait is both simple and complex: it is simple conceptually because its single hallmark is an excess of adipose tissue. However, it is complex because not all adipose tissue is the same. It is stored in depots which differ in location, size and function [13, 14, 70] and each depot has a different genetic architecture [15] and pattern of gene expression [71, 72]. Further complexities arise because adipose tissue is hard to measure directly, and each measurement method yields different results [73]. Here we chose to study one adipose depot which we measured directly by necropsy. This is a simple measurement method and our expectation was that its genetic architecture would be less complex than for whole-body obesity. We specifically chose the gonadal rather than the inguinal, subscapular, mesenteric, retroperitoneal or pericardial adipose depot because it is the heaviest [13, 14, 70] and a proxy for overall adiposity [74, 75]. However, despite all these complexities, both mouse and human genetic approaches point to the same underlying mammalian biology: QTL regions found here contain many mouse orthologues for obesity genes identified by human genome wide association studies.

We began the construction congenic mice guided by mapping results from two intercross populations. We also bred reciprocal consomics which helped us to define the genetic architecture [11] and they also served as a source of breeder mice for the construction of the congenic strains. Building on the information from the consomic mice study [11], we learned that single *Adip20* on chromosome 9 could not explain the observed results from the reciprocal consomic strains [11]. The results explained by the congenic mice studied here confirmed the more general results from the consomic strains that there were multiple QTL with opposing effects.

Within the four QTL regions we identified, there are 429 protein-coding genes [22]. When plan to evaluate these genes and variants for their role in obesity, there is a technical gap between the available and ideal testing methods. The most common available method is the total elimination of each gene (e.g., gene knockout) and quantification of knockout vs control mice. However, this method has a serious limitation as an approach to study obesity. Large-scale knockout surveys indicate that inactivating mutations affect early embryonic growth for nearly half of genes tested [76], and about a third of genes affect body composition in adult mice [77, 78]. This method has poor specify, so we cannot assume that if knockouts differ from controls in body composition, e.g., [79], than the target gene is causal. Likewise, bioinformatics methods to evaluate functional variants are also not ideal because ~10% of these genes have potentially functional variants. Furthermore, we cannot completely exclude any of the thousands of observed variants because evaluating potential function with currently available informatics methods remains imperfect. For complex traits, the challenge is now to find new ways to winnow a large number of variants to only a few or to find a way to test many variants and their combinations rapidly.

While congenic mapping methods were useful in identifying additional adiposity QTLs on mouse chromosome 9, there are at least four limitations to consider when interpreting the

results. The study of male mice exclusively we mentioned earlier. A second limitation is the residual heterozygosity within the congenic strains that we confirmed through genotyping. The amount was low relative to the number of backcross cycles because we used marker assisted breeding, but still it may have contributed to experimental noise. To put this limitation in a broader context, we have learned recently from whole genome sequencing studies that will not ensure that all members of a particular inbred strain are completely genetically identical [80]. Whether variants among members of the same inbred strain are technical artifacts or represent true diversity is controversial, but if true may explain in part the rapidly divergence in body weight during selective breeding of inbred mouse strains [81]. A third limitation of this study is that our congenic breeding paradigm only allowed us to detect effects of the B6/B6 vs 129/B6 genotypes but we may have found larger effect sizes or additional QTL by including mice that were homozygous for the donor region. The fourth limitation is that the congenic breakpoints were concentrated more in the middle regions of the chromosome and we may have missed additional QTL in the proximal region where there were fewer breakpoints.

We used three methods to evaluate causal genes but no single gene emerged as a highly prioritized candidate within any QTL region. This lack of convergence among methods may be due in part to the differing assumptions of each. For instance, microarray approach we used here assumes the causal variation affects gene expression in the gonadal adipose depot of adult mice but the actual causal variants may not affect gene expression at all or may act in a different tissue or at a different time in development. Likewise, the analysis of DNA sequence we used here assumes that causal sequence variation creates missense or loss of function effects but instead the variation may be in regulatory regions rather than within coding sequences [82]. These points made, there was some convergence among methods. Specifically, the *OSBPL10* gene was identified by a human genome-wide association study of body mass index [83] and the mouse orthologue of this gene which is within the QTL4 region

had a missense variant between the 129 and B6 mouse strains. Similarly, mouse gonadal adipose tissue expresses different amounts of *Dixdc1* and *Sik2* mRNA depending on QTL2 genotype and each of the corresponding genes has two predicted missense variants. These results provide some direction in the future evaluation of candidate genes.

This study design successfully identified linked multiple QTLs on chromosome 9 that contribute to genetic diversity in mouse adiposity. Our results highlight the advantages of congenic strains as a tool to explore the genetic architecture of complex traits. One potential next step would be the study of an advanced intercross population created from the inbred parental strains. Using that approach, the optimal haplotypes at each QTL location identified here by the convergence of results from multiple strains and mapping populations could be reconstituted and studied in a single mapping population [84]. However, the main drawback of this approach is that it is resource intensive and would take years to breed the mice. Another approach would be to use an established mapping resources like the "Collaborative Cross" [84]. This approach is appealing because the mapping population is immediately available and feasible because the QTL detected here appear to be common [50, 59, 85-90] and therefore more likely to be captured in this cross. The drawback is that the inclusion of additional QTLs from the others parental strains beyond those studied here would likely cause small or perhaps large shifts in genetic architecture. Thus, we reiterate the need for new and effective methods to study mammalian traits with complex architecture.

Acknowledgements

We gratefully acknowledge the assistance with animal breeding of Rebecca James, Liang-Dar (Daniel) Hwang, Zakiyyah Smith, Matt Kirkey, Amy Colihan, and Laurie Pippett. We also acknowledge Richard Copeland and the consistent high-quality assistance of the animal care staff at the Monell Chemical Senses Center and thank them for their service. Michael G. Tordoff and Gary K. Beauchamp commented on a draft of the manuscript. Joseph H. Nadeau provided valuable advice on analytical approaches and manuscript preparation. We thank the two anonymous reviewers for their constructive comments on this manuscript.

Funding

The National Institutes of Health grant R01 DK094759, R01 DK058797, P30 DC011735, OD018125, RR025607, RR026752 and institutional funds from the Monell Chemical Senses Center funded this work including genotyping and the purchase of equipment. The Center for Inherited Disease Research though the auspices of the National Institutes of Health provided genotyping services.

Accession ID

We used mice for these experiments, NCBI Taxon ID 10090.

Electronic Resources

http://www.cidr.jhmi.edu/nih/Completed_Projects_Report_June15.pdf

Table 1. Characteristics of congenicmice by strains

Strain[a]	N	Age at necropsy (days)	
		Range	Mean±SD
1	113	175-187	180±2
1.1	176	162-184	180±2
1.1.1	3	180	180±0
1.2	14	180-182	181±1
3	175	177-190	180±2
3.1	120	178-182	180±1
3.1.1	106	178-186	180±1
3.1.1.1	127	179-184	181±1
3.1.1.2	34	179-181	180±1
3.1.1.3	14	179-181	180±1
3.1.1.4	63	103[b]-193	160±29
3.1.2	21	180-183	181±1
3.1.3	6	178-183	181±2
3.1.4	11	179-181	180±1
3.1.4.1	26	179-191	181±3
4	119	175-188	180±2
4.1	44	179-231	182±8
4.1a	22	177-190	180±3
4.2	16	180-181	180±0
4.3	18	179-183	181±1
4.4	61	178-193	181±3
4.5	4	179-181	180±1

[a]Substrain IDs. SD=0 indicates less than one day.
[b]We necropsied 10 younger mice with age ranging from 103 to 124 days.

Adiposity QTL *Adip20*

Table 2. Human genome-wide associations within mouse QTLs for adiposity and body mass index

QTL	Mouse QTL location	Human region	Adiposity	Body mass index
1	chr9:42779420-44142555	chr11:119308720-120693788	None	None
2	chr9:48789608-53884418	chr11:107691025-114109156	*FDX1*	*C11orf53*
			ARHGAP20	*NCAM1*
3	chr9:54242579-54286770	chr15:51295990-51341931	*None*	*DMXL2*
4	chr9:108915010-118915010	chr3:27712199-48621406	*PDCD6IP*	*OSBPL10*
			TRAK1	*LOC101928114*
				CCK

This table lists chromosome: bp locations for mouse (GRCm38; mm10) and human (GRCh38). We obtained human orthologous regions by the UCSC genome converter [91]. “Adiposity” and “Body mass index” columns contain Human Gene Nomenclature Committee gene symbols.

Figure captions

Figure 1. The location of the gonadal adipose depot in a male mouse.

Figure 2. Adiposity QTLs on chromosome 9 are detectable in all congenic mice. (**A**) The x-axis is the location of the markers (see **Supplemental Table 1**) in Mb on mouse chromosome 9 (mChr9); the y-axis is the –log p-values (black line) obtained in a general linear model analysis with body weight as a covariate (red line, significant threshold; grey line, suggestive). We defined the QTL confidence intervals (blue line) by two units of –log10 p-value drop from the peak. (**B**) The y-axis is the average weight of the gonadal adipose depot by genotype (B6/B6, black; B6/129, grey) of the most associated marker (i.e., the marker with the lowest p value); *differences between genotypes ($p<0.0001$, post hoc Fisher's LSD tests). The panel (**C**) shows the Cohen's *D* effect size (green bars) of the comparison between B6/B6 and 129/B6 for the peak marker *rs3723670.*

Figure 3. (**A**) Minimum spanning tree (MST). (**B**) Mean and SEM (standard error of the mean) by strain for the gonadal adipose depot weight. N = number of mice in each group. P-values are for least-significant-difference t-tests for each sequential comparison; red text indicates p-values that met the threshold ($p<0.05$). For the comparisons of two strains, the first strain was either greater (>), less than (<), or equal (=) to the second strain in gonadal adipose depot weight. "Model" lists QTLs contained within the donor fragment of each congenic strain suggested by the sequential analysis. (**C**) Congenic strains (numbers show strain IDs; "Host" = combined group of littermates without the donor fragment) and genotypes for informative markers (A = B6/B6; H = 129/B6; X = missing data). QTLs are shown at the bottom as black boxes; arrows show the direction of effect (e.g., ↑ indicates that the QTL allele from the 129 strain increases

the trait value). The data support the presence of four QTLs; we reported the detailed logic for this conclusion in **Supplemental Text 2**.

Figure 4. Filtering on a volcano plot of the microarray data analysis of the Experiment 1 (A) and Experiment 2 (B). The statistical comparison of the expression of genes within the donor fragment region from 42.6 to 58.3 Mb (congenic strain 4, **Figure 3C**) from the gonadal adipose tissue between heterozygous mice (129/B6) versus littermates without 129 donor fragment (B6/B6). The customized volcano plot depicts the estimated fold-change (x-axis) and statistical significance ($-\log_{10}$P-value, y-axis). Each point represents one gene. The green point (see A) shows gene *Dixdc1* with Log_2FoldChange>1 and FDR <0.05. We summarize the details of these filtered results in **Supplemental Table 11.**

Figure 5. The logical relations of among the candidate gene evidence from missense genetic variation, human adiposity or body mass index orthologues and differential gene expression. The unique genes (n=48) for missenses genetic variation within the four QTL regions are shown in the **Supplemental Table 9**. The human adipose or body mass index orthologous genes (n=10) are summarized in the **Table 2,** and the differentially expressed genes (n=11) flited in the microarray experiments are shown the **Supplemental Table 11**.

References

1. Reed DR, Bachmanov AA, Tordoff MG. Forty mouse strain survey of body composition. Physiol Behav. 2007;91(5):593-600. PubMed PMID: 17493645.

2. Reed DR, Duke FF, Ellis HK, Rosazza MR, Lawler MP, Alarcon LK, et al. Body fat distribution and organ weights of 14 common strains and a 22-strain consomic panel of rats. Physiol Behav. 2011;103:523-9. Epub 2011/04/21. doi: 10.1016/j.physbeh.2011.04.006. PubMed PMID: 21504752.

3. Fried SK, Lee MJ, Karastergiou K. Shaping fat distribution: New insights into the molecular determinants of depot- and sex-dependent adipose biology. Obesity (Silver Spring). 2015;23(7):1345-52. doi: 10.1002/oby.21133. PubMed PMID: 26054752; PubMed Central PMCID: PMCPMC4687449.

4. Eppig JT, Bult CJ, Kadin JA, Richardson JE, Blake JA, Anagnostopoulos A, et al. The Mouse Genome Database (MGD): from genes to mice--a community resource for mouse biology. Nucleic Acids Res. 2005;33(Database issue):D471-5. PubMed PMID: 15608240.

5. Drinkwater NR, Gould MN. The long path from QTL to gene. PLoS Genet. 2012;8(9):e1002975. doi: 10.1371/journal.pgen.1002975. PubMed PMID: 23049490; PubMed Central PMCID: PMCPMC3462162.

6. El-Sayed Moustafa JS, Froguel P. From obesity genetics to the future of personalized obesity therapy. Nat Rev Endocrinol. 2013;9(7):402-13. doi: 10.1038/nrendo.2013.57. PubMed PMID: 23529041.

7. Reed DR, Li X, McDaniel AH, Lu K, Li S, Tordoff MG, et al. Loci on chromosomes 2, 4, 9, and 16 for body weight, body length, and adiposity identified in a

genome scan of an F2 intercross between the 129P3/J and C57BL/6ByJ mouse strains. Mamm Genome. 2003;14(5):302-13. PubMed PMID: 12856282.

8. Reed DR, McDaniel AH, Li X, Tordoff MG, Bachmanov AA. Quantitative trait loci for individual adipose depot weights in C57BL/6ByJ x 129P3/J F(2) mice. Mamm Genome. 2006;17(11):1065-77. PubMed PMID: 17103053.

9. Bachmanov AA, Reed DR, Tordoff MG, Price RA, Beauchamp GK. Nutrient preference and diet-induced adiposity in C57BL/6ByJ and 129P3/J mice. Physiol Behav. 2001;72:603-13.

10. Shao H, Sinasac DS, Burrage LC, Hodges CA, Supelak PJ, Palmert MR, et al. Analyzing complex traits with congenic strains. Mamm Genome. 2010;21(5-6):276-86. doi: 10.1007/s00335-010-9267-5. PubMed PMID: 20524000; PubMed Central PMCID: PMCPMC3805105.

11. Lin C, Fesi BD, Marquis M, Bosak NP, Theodorides ML, Avigdor M, et al. Body Composition QTLs Identified in Intercross Populations Are Reproducible in Consomic Mouse Strains. PLoS One. 2015;10(11):e0141494. doi: 10.1371/journal.pone.0141494. PubMed PMID: 26551037; PubMed Central PMCID: PMCPMC4638354.

12. Dietrich W, Katz H, Lincoln SE, Shin HS, Friedman J, Dracopoli NC, et al. A genetic map of the mouse suitable for typing intraspecific crosses. Genetics. 1992;131(2):423-47. Epub 1992/06/01. PubMed PMID: 1353738; PubMed Central PMCID: PMC1205016.

13. Cinti S. The adipose organ. Milano: Editrice Kurtis; 1999.

14. Hayakawa T, Yamasita H, Iwaki T. A Color Atlas of Sectional Anatomy of the Mouse: Braintree Scientific Inc; 2001.

15. McDaniel AH, Li X, Tordoff MG, Bachmanov AA, Reed DR. A locus on mouse Chromosome 9 (Adip5) affects the relative weight of the gonadal but not retroperitoneal adipose depot. Mamm Genome. 2006;17(11):1078-92. PubMed PMID: 17103052.

16. Delignette-Muller M, Pouillot, R., Denis, J., and Dutang, C. . fitdistrplus: Help to Fit of a Parametric Distribution to Non-Censored or Censored Data. R package. 2014.

17. Cohen J. Statistical power analysis for the behavioral sciences. 2nd ed. Hillsdale, N.J.: L. Erlbaum Associates; 1988. xxi, 567 p. p.

18. Lander E, Kruglyak L. Genetic dissection of complex traits: guidelines for interpreting and reporting linkage findings. Nat Genet. 1995;11:241-7.

19. Shao H, Sinasac DS, Burrage LC, Hodges CA, Supelak PJ, Palmert MR, et al. Analyzing complex traits with congenic strains. Mammalian genome : official journal of the International Mammalian Genome Society. 2010;21(5-6):276-86. Epub 2010/06/05. doi: 10.1007/s00335-010-9267-5. PubMed PMID: 20524000.

20. Fontenla M. optrees: Optimal Trees in Weighted Graphs. 1.0 ed. CRAN2014.

21. Csardi G, Nepusz T. The igraph software package for complex network research. InterJournal, Complex Systems 16952006.

22. Mus musculus (laboratory mouse) genome view [Internet]. National Center for Biotechnology Information 2015 [cited 10/7/2016]. Available from: https://www.ncbi.nlm.nih.gov/projects/mapview/map_search.cgi?taxid=10090&build=105.0.

23. Mouse Genomes Project - Query SNPs, indels or SVs [Internet]. 2011 [cited 10/7/2016]. Available from: http://www.sanger.ac.uk/sanger/Mouse_SnpViewer/rel-1505.

24. Keane TM, Goodstadt L, Danecek P, White MA, Wong K, Yalcin B, et al. Mouse genomic variation and its effect on phenotypes and gene regulation. Nature.

2011;477(7364):289-94. Epub 2011/09/17. doi: 10.1038/nature10413. PubMed PMID: 21921910.

25. Yalcin B, Wong K, Agam A, Goodson M, Keane TM, Gan X, et al. Sequence-based characterization of structural variation in the mouse genome. Nature. 2011;477(7364):326-9. doi: 10.1038/nature10432. PubMed PMID: 21921916; PubMed Central PMCID: PMCPMC3428933.

26. Anonymous. SIFT web server: predicting effects of amino acid substitutions on proteins: Nucleic Acids Research; 2012 [cited 2016 10/7/2016]. August 15th 2015:[W542-7 (Link)]. Available from: http://siftdna.org/www/SIFT_dbSNP.html.

27. Anonymous. dbSNP, Single Nucleotide Polymorphisms; http://www.ncbi.nlm.nih.gov/SNP/index.html: National Center for Biotechnology Information; 2016 [cited 2016 10/7/2016]. Available from: http://www.ncbi.nlm.nih.gov/SNP/index.html.

28. GWAS Catalog: the NHGRI-EBI Catalog of published genome-wide association studies [Internet]. European Molecular Biology Laboratory. 2015 [cited 10/7/2016]. Available from: http://www.ebi.ac.uk/gwas/.

29. de Buhr MF, Mahler M, Geffers R, Hansen W, Westendorf AM, Lauber J, et al. Cd14, Gbp1, and Pla2g2a: three major candidate genes for experimental IBD identified by combining QTL and microarray analyses. Physiol Genomics. 2006;25(3):426-34. doi: 10.1152/physiolgenomics.00022.2005. PubMed PMID: 16705022.

30. de Ledesma AM, Desai AN, Bolivar VJ, Symula DJ, Flaherty L. Two new behavioral QTLs, Emo4 and Reb1, map to mouse Chromosome 1: Congenic strains and candidate gene identification studies. Mamm Genome. 2006;17(2):111-8. doi: 10.1007/s00335-005-0107-y. PubMed PMID: 16465591.

31. Stylianou IM, Clinton M, Keightley PD, Pritchard C, Tymowska-Lalanne Z, Bunger L, et al. Microarray gene expression analysis of the Fob3b obesity QTL identifies positional candidate gene Sqle and perturbed cholesterol and glycolysis pathways. Physiol Genomics. 2005;20(3):224-32. doi: 10.1152/physiolgenomics.00183.2004. PubMed PMID: 15598878.

32. Benjamini Y, Hochberg Y. Controlling the false discovery rate: A practical and powerful approach to multiple testing. Journal of the Royal Statistical Society Series B (Methodological). 1995;57(1):289-300.

33. Yick CY, Zwinderman AH, Kunst PW, Grunberg K, Mauad T, Dijkhuis A, et al. Transcriptome sequencing (RNA-Seq) of human endobronchial biopsies: asthma versus controls. Eur Respir J. 2013;42(3):662-70. doi: 10.1183/09031936.00115412. PubMed PMID: 23314903.

34. Nicholas Lewin-Koh EP, Eric Archer, Adrian Baddeley, Nick Bearman, Hans-Jörg Bibiko, Steven Brey, Jonathan Callahan, German Carrillo, Stéphane Dray, David Forrest, Michael Friendly, Patrick Giraudoux, Duncan Golicher. Tools for Reading and Handling Spatial Objects. R Package. 2017.

35. Dixon JR, Selvaraj S, Yue F, Kim A, Li Y, Shen Y, et al. Topological domains in mammalian genomes identified by analysis of chromatin interactions. Nature. 2012;485(7398):376-80. doi: 10.1038/nature11082. PubMed PMID: 22495300; PubMed Central PMCID: PMCPMC3356448.

36. Reed DR. Adip20. 2016.

37. Zhang Y, Proenca R, Maffei M, Barone M, Leopold L, Friedman JM. Positional cloning of the mouse obese gene and its human homologue. Nature. 1994;372(6505):425-32. doi: 10.1038/372425a0. PubMed PMID: 7984236.

38. Tartaglia LA, Dembski M, Weng X, Deng N, Culpepper J, Devos R, et al. Identification and expression cloning of a leptin receptor, OB-R. Cell. 1995;83(7):1263-71. PubMed PMID: 8548812.

39. Kleyn PW, Fan W, Kovats SG, Lee JJ, Pulido JC, Wu Y, et al. Identification and characterization of the mouse obesity gene tubby: a member of a novel gene family. Cell. 1996;85(2):281-90. PubMed PMID: 8612280.

40. Noben-Trauth K, Naggert JK, North MA, Nishina PM. A candidate gene for the mouse mutation tubby. Nature. 1996;380(6574):534-8. doi: 10.1038/380534a0. PubMed PMID: 8606774.

41. Bultman SJ, Michaud EJ, Woychik RP. Molecular characterization of the mouse agouti locus. Cell. 1992;71(7):1195-204. PubMed PMID: 1473152.

42. Coleman DL. Obese and diabetes: two mutant genes causing diabetes-obesity syndromes in mice. Diabetologia. 1978;14(3):141-8. PubMed PMID: 350680.

43. Jerez-Timaure NC, Kearney F, Simpson EB, Eisen EJ, Pomp D. Characterization of QTL with major effects on fatness and growth on mouse chromosome 2. Obes Res. 2004;12(9):1408-20. Epub 2004/10/16. doi: 10.1038/oby.2004.177. PubMed PMID: 15483205.

44. Ishimori N, Li R, Kelmenson PM, Korstanje R, Walsh KA, Churchill GA, et al. Quantitative trait loci that determine plasma lipids and obesity in C57BL/6J and 129S1/SvImJ inbred mice. J Lipid Res. 2004;45(9):1624-32. PubMed PMID: 15210844.

45. Cheverud JM, Ehrich TH, Hrbek T, Kenney JP, Pletscher LS, Semenkovich CF. Quantitative trait loci for obesity- and diabetes-related traits and their dietary responses to high-fat feeding in LGXSM recombinant inbred mouse strains. Diabetes. 2004;53(12):3328-36. PubMed PMID: 15561968.

46. Taylor BA, Wnek C, Schroeder D, Phillips SJ. Multiple obesity QTLs identified in an intercross between the NZO (New Zealand obese) and the SM (small) mouse strains. Mamm Genome. 2001;12(2):95-103. PubMed PMID: 11210195.

47. Ogino T, Wei S, Wei K, Moralejo DH, Kose H, Mizuno A, et al. Genetic evidence for obesity loci involved in the regulation of body fat distribution in obese type 2 diabetes rat, OLETF. Genomics. 2000;70(1):19-25. PubMed PMID: 11087657.

48. Horvat S, Bunger L, Falconer VM, Mackay P, Law A, Bulfield G, et al. Mapping of obesity QTLs in a cross between mouse lines divergently selected on fat content. Mamm Genome. 2000;11(1):2-7. PubMed PMID: 10602985.

49. Brockmann GA, Kratzsch J, Haley CS, Renne U, Schwerin M, Karle S. Single QTL effects, epistasis, and pleiotropy account for two-thirds of the phenotypic F(2) variance of growth and obesity in DU6i x DBA/2 mice. Genome Res. 2000;10(12):1941-57. PubMed PMID: 11116089.

50. Taylor BA, Tarantino LM, Phillips SJ. Gender-influenced obesity QTLs identified in a cross involving the KK type II diabetes-prone mouse strain. Mamm Genome. 1999;10(10):963-8. PubMed PMID: 10501964.

51. Suto J, Matsuura S, Imamura K, Yamanaka H, Sekikawa K. Genetics of obesity in KK mouse and effects of A(y) allele on quantitative regulation. Mamm Genome. 1998;9(7):506-10. Epub 1998/07/10. PubMed PMID: 9657845.

52. Keightley PD, Morris KH, Ishikawa A, Falconer VM, Oliver F. Test of candidate gene--quantitative trait locus association applied to fatness in mice. Heredity. 1998;81 (Pt 6):630-7. PubMed PMID: 9885188.

53. Brockmann GA, Haley CS, Renne U, Knott SA, Schwerin M. Quantitative trait loci affecting body weight and fatness from a mouse line selected for extreme high growth. Genetics. 1998;150(1):369-81. PubMed PMID: 9725853.

54. York B, Lei K, West DB. Inherited non-autosomal effects on body fat in F2 mice derived from an AKR/J x SWR/J cross. Mamm Genome. 1997;8(10):726-30. Epub 1997/10/08. PubMed PMID: 9321464.

55. Taylor BA, Phillips SJ. Obesity QTLs on mouse chromosomes 2 and 17. Genomics. 1997;43(3):249-57. PubMed PMID: 9268627.

56. Lembertas AV, Perusse L, Chagnon YC, Fisler JS, Warden CH, Purcell-Huynh DA, et al. Identification of an obesity quantitative trait locus on mouse chromosome 2 and evidence of linkage to body fat and insulin on the human homologous region 20q. J Clin Invest. 1997;100(5):1240-7. PubMed PMID: 9276742.

57. York B, Lei K, West DB. Sensitivity to dietary obesity linked to a locus on chromosome 15 in a CAST/Ei x C57BL/6J F2 intercross. Mamm Genome. 1996;7(9):677-81. Epub 1996/09/01. PubMed PMID: 8703121.

58. Taylor BA, Phillips SJ. Detection of obesity QTLs on mouse chromosomes 1 and 7 by selective DNA pooling. Genomics. 1996;34(3):389-98. Epub 1996/06/15. doi: 10.1006/geno.1996.0302. PubMed PMID: 8786140.

59. West DB, Waguespack J, York B, Goudey-Lefevre J, Price RA. Genetics of dietary obesity in AKR/J x SWR/J mice: segregation of the trait and identification of a linked locus on chromosome 4. Mamm Genome. 1994;5(9):546-52. PubMed PMID: 8000138.

60. West DB, Goudey-Lefevre J, York B, Truett GE. Dietary obesity linked to genetic loci on chromosomes 9 and 15 in a polygenic mouse model. J Clin Invest. 1994;94(4):1410-6. PubMed PMID: 7929816.

61. Gularte-Merida R, Farber CR, Verdugo RA, Islas-Trejo A, Famula TR, Warden CH, et al. Overlapping mouse subcongenic strains successfully separate two linked body fat QTL on distal MMU 2. BMC Genomics. 2015;16:16. Epub 2015/01/24. doi:

10.1186/s12864-014-1191-8. PubMed PMID: 25613955; PubMed Central PMCID: PMC4308015.

62. Farber CR, Medrano JF. Dissection of a genetically complex cluster of growth and obesity QTLs on mouse chromosome 2 using subcongenic intercrosses. Mamm Genome. 2007;18(9):635-45. doi: 10.1007/s00335-007-9046-0. PubMed PMID: 17694346.

63. Randall JC, Winkler TW, Kutalik Z, Berndt SI, Jackson AU, Monda KL, et al. Sex-stratified genome-wide association studies including 270,000 individuals show sexual dimorphism in genetic loci for anthropometric traits. PLoS genetics. 2013;9(6):e1003500. Epub 2013/06/12. doi: 10.1371/journal.pgen.1003500. PubMed PMID: 23754948; PubMed Central PMCID: PMC3674993.

64. Farber CR, Medrano JF. Fine mapping reveals sex bias in quantitative trait loci affecting growth, skeletal size and obesity-related traits on mouse chromosomes 2 and 11. Genetics. 2007;175(1):349-60. PubMed PMID: 17110492.

65. Zhao W, Ma C, Cheverud JM, Wu R. A unifying statistical model for QTL mapping of genotype x sex interaction for developmental trajectories. Physiol Genomics. 2004;19(2):218-27. PubMed PMID: 15304622.

66. Clayton JA, Collins FS. Policy: NIH to balance sex in cell and animal studies. Nature. 2014;509(7500):282-3. PubMed PMID: 24834516.

67. Cheverud JM, Routman EJ, Duarte FA, van Swinderen B, Cothran K, Perel C. Quantitative trait loci for murine growth. Genetics. 1996;142(4):1305-19. Epub 1996/04/01. PubMed PMID: 8846907; PubMed Central PMCID: PMC1207127.

68. Wolf JB, Cheverud JM, Roseman C, Hager R. Genome-wide analysis reveals a complex pattern of genomic imprinting in mice. PLoS Genet. 2008;4(6):e1000091. PubMed PMID: 18535661.

69. Lawson HA, Cheverud JM, Wolf JB. Genomic imprinting and parent-of-origin effects on complex traits. Nat Rev Genet. 2013;14(9):609-17. doi: 10.1038/nrg3543. PubMed PMID: 23917626; PubMed Central PMCID: PMCPMC3926806.

70. Pond CM. The fats of life. Cambridge ; New York: Cambridge University Press; 1998. 337 p.

71. Yamamoto Y, Gesta S, Lee KY, Tran TT, Saadatirad P, Kahn CR. Adipose depots possess unique developmental gene signatures. Obesity (Silver Spring). 2010;18(5):872-8. PubMed PMID: 20111017.

72. Gesta S, Bluher M, Yamamoto Y, Norris AW, Berndt J, Kralisch S, et al. Evidence for a role of developmental genes in the origin of obesity and body fat distribution. Proc Natl Acad Sci USA. 2006;103(17):6676-81. PubMed PMID: 16617105.

73. Halldorsdottir S, Carmody J, Boozer CN, Leduc CA, Leibel RL. Reproducibility and accuracy of body composition assessments in mice by dual energy x-ray absorptiometry and time domain nuclear magnetic resonance. Int J Body Compos Res. 2009;7(4):147-54. PubMed PMID: 21909234; PubMed Central PMCID: PMCPMC3169293.

74. Fesi B, Marquis M, Lysenko A, James R, Lin C, Bachmanov A, et al. Refining fat phenotypes: multiple measures of body composition in 1,386 mice. Kroc Lecture and Symposium; University of Pennsylvania2013.

75. Eisen EJ, Coffey MT. Correlated responses in body composition based on selection for different indicator traits in mice. J Anim Sci. 1990;68(11):3557-62. Epub 1990/11/01. PubMed PMID: 2262408.

76. Dickinson ME, Flenniken AM, Ji X, Teboul L, Wong MD, White JK, et al. High-throughput discovery of novel developmental phenotypes. Nature. 2016;537(7621):508-14. doi: 10.1038/nature19356. PubMed PMID: 27626380.

77. White JK, Gerdin AK, Karp NA, Ryder E, Buljan M, Bussell JN, et al. Genome-wide generation and systematic phenotyping of knockout mice reveals new roles for many genes. Cell. 2013;154(2):452-64. Epub 2013/07/23. doi: 10.1016/j.cell.2013.06.022. PubMed PMID: 23870131; PubMed Central PMCID: PMC3717207.

78. Reed DR, Lawler MP, Tordoff MG. Reduced body weight is a common effect of gene knockout in mice. BMC Genet. 2008;9(1):4. PubMed PMID: 18182103.

79. Koscielny G, Yaikhom G, Iyer V, Meehan TF, Morgan H, Atienza-Herrero J, et al. The International Mouse Phenotyping Consortium Web Portal, a unified point of access for knockout mice and related phenotyping data. Nucleic Acids Res. 2014;42(Database issue):D802-9. doi: 10.1093/nar/gkt977. PubMed PMID: 24194600; PubMed Central PMCID: PMCPMC3964955.

80. Oey H, Isbel L, Hickey P, Ebaid B, Whitelaw E. Genetic and epigenetic variation among inbred mouse littermates: identification of inter-individual differentially methylated regions. Epigenetics Chromatin. 2015;8:54. doi: 10.1186/s13072-015-0047-z. PubMed PMID: 26692901; PubMed Central PMCID: PMCPMC4676890.

81. Keightley PD. Genetic basis of response to 50 generations of selection on body weight in inbred mice. Genetics. 1998;148(4):1931-9. PubMed PMID: 9560406.

82. Soccio RE, Chen ER, Rajapurkar SR, Safabakhsh P, Marinis JM, Dispirito JR, et al. Genetic Variation Determines PPARgamma Function and Anti-diabetic Drug Response In Vivo. Cell. 2015;162(1):33-44. doi: 10.1016/j.cell.2015.06.025. PubMed PMID: 26140591; PubMed Central PMCID: PMCPMC4493773.

83. Boardman JD, Domingue BW, Blalock CL, Haberstick BC, Harris KM, McQueen MB. Is the gene-environment interaction paradigm relevant to genome-wide studies? The case of education and body mass index. Demography. 2014;51(1):119-39. doi:

10.1007/s13524-013-0259-4. PubMed PMID: 24281739; PubMed Central PMCID: PMCPMC4035460.

84. Buchner DA, Nadeau JH. Contrasting genetic architectures in different mouse reference populations used for studying complex traits. Genome Res. 2015;25(6):775-91. doi: 10.1101/gr.187450.114. PubMed PMID: 25953951; PubMed Central PMCID: PMCPMC4448675.

85. Cheverud JM, Vaughn TT, Pletscher LS, Peripato AC, Adams ES, Erikson CF, et al. Genetic architecture of adiposity in the cross of LG/J and SM/J inbred mice. Mamm Genome. 2001;12(1):3-12. PubMed PMID: 11178736.

86. Stylianou IM, Korstanje R, Li R, Sheehan S, Paigen B, Churchill GA. Quantitative trait locus analysis for obesity reveals multiple networks of interacting loci. Mamm Genome. 2006;17(1):22-36. PubMed PMID: 16416088.

87. Mehrabian M, Wen PZ, Fisler J, Davis RC, Lusis AJ. Genetic loci controlling body fat, lipoprotein metabolism, and insulin levels in a multifactorial mouse model. J Clin Invest. 1998;101(11):2485-96. PubMed PMID: 9616220.

88. Farber CR, FArber EA, De Vera V, Gluarte R, Castellani LW, Lusis AJ, et al., editors. Mouse chromosome 9 congenic-derived F2 intercrosses refine the location of a major obesity quantitative trait locus (QTL) (Carfhg2) and uncover a distinct QTL influencing plasma cholesterol (Cholhg1). Keystone; 2007; Keystone, Colorado.

89. Gordon RR, Hunter KW, Sorensen P, Pomp D. Genotype x diet interactions in mice predisposed to mammary cancer. I. Body weight and fat. Mamm Genome. 2008. PubMed PMID: 18286334.

90. Yaguchi H, Togawa K, Moritani M, Itakura M. Identification of candidate genes in the type 2 diabetes modifier locus using expression QTL. Genomics. 2005;85(5):591-9. Epub 2005/04/12. doi: 10.1016/j.ygeno.2005.01.006. PubMed PMID: 15820311.

91. Kent WJ, Sugnet CW, Furey TS, Roskin KM, Pringle TH, Zahler AM, et al. The human genome browser at UCSC. Genome Res. 2002;12(6):996-1006. PubMed PMID: 12045153.

Supporting Information

S1 Table. Markers used for genotyping and their physical positions (GRCm38, mm10) on chromosome 9

S2 Table. List of mice with tumors or otherwise excluded from analysis

Weight=Body weight in grams; Length, body length in centimeters, gonadal adipose depot weight at the time of dissection in grams; tumor location, weights if available.

S3 Table. Statistic descriptive and normality tests of gonadal adipose depot weight in a combined congenic population

S4 Table. Weight of gonadal depot and body weight (BW) of congenic mice with different genotypes of donor regions

[a]Donor region genotype: Host = B6/B6; Donor = 129/B6.

[b]Donor region size: NA = mice without donor region; Partial = mice that inherited partial-length (due to a recombination event) donor region from father; Full = mice that inherited full-length donor region from father.

S5 Table. Genotypes and phenotypes of the 12 congenic strains (with numbers of mice ≥12/strain, and all mice having full-length donor regions).

Column headings show substrain IDs of congenic strains. We show here only markers informative for breakpoints of the donor regions. A=B6/B6 genotype; H=129/B6 genotype; X=data are not available. Based on analysis of gonadal depot weight (see **Supplemental Tables 4 and 6**), strains were identified as Adip20+ (shaded; strains with significant differences between mice with B6/B6 and 129/B6 genotypes) or Adip20- (no shading; strains with no significant differences between mice with B6/B6 and 129/B6 genotypes). The far right column "Shared region" indicates whether a QTL-containing

region is shared only by Adip20+ but not by Adip20- strains (i.e., whether a marker genotype is H in all Adip20+ strains and A in all Adip20- strains). None of the regions of chromosome 9 has met this criterion.

S6 Table. Analysis of gonadal depot weight in the 12 congenic strains (with numbers of mice ≥12/strain, and all mice having full-length donor regions).

N=Numbers of mice in the groups with ("donor", genotype 129/B6) and without ("host", genotype B6/B6) a donor region. The "donor" group includes only mice with full-length length donor regions. We show an analysis of mice with both partial and full-length donor regions in **Supplemental Table 8** and the means and SD for each genotype groups in **Supplemental Table 4.**

S7 Table. Genotypes and phenotypes of the congenic strains (with any numbers of mice, including both partial and full-length donor regions).

This analysis excluded three strains (1.1.1, 3.1.3, 4.5) with a small sample size shaded in light grey. Other details are the same as from Supplemental Table 5 except that almost all congenic strains are included.

S8 Table. Analysis of gonadal depot weight in the congenic strains (with any numbers of mice, including both partial and full-length donor regions).

Details are the same as from Supplemental Table 6 except that almost all congenic strains are included. NA=not applicable (i.e., there were too few mice per group for analysis, which indicated in light grey in Supplemental Table 7).

S9 Table. Sorting Intolerant From Tolerant (SIFT) prediction of missense and stop codon gain/loss sequence variants of genes residing within the 4 adiposity QTL regions on chromosome 9

S10 Table. Summary of the mouse adiposity QTLs on chromosome 9

Type=mapping population, Con=congenic, Overlap refers to QTL1 to 4 as identified in the accompany text. Approach =method of estimating confidence interval. Ref=reference.

S11 Table. Filtering of microarray data to identify reproducible candidate genes

S1 Text. Congenic analysis using the common segment method

S2 Text. Detailed logic for the interpretation of the congenic data

S1 Figure. We tested the distribution of the gonadal adipose depot weight data for normality and we summarize the parameters of the model-fitting untransformed and log-transformed data in **Supplemental Table 3**.

S2 Figure. Pearson correlations between (A) gonadal adipose depot and body weight, (B) gonadal adipose depot and age as well as (C) body weight and age of all congenic mice. Gonadal=Gonadal adipose depot in grams; BW=body weight in grams; Age in days.

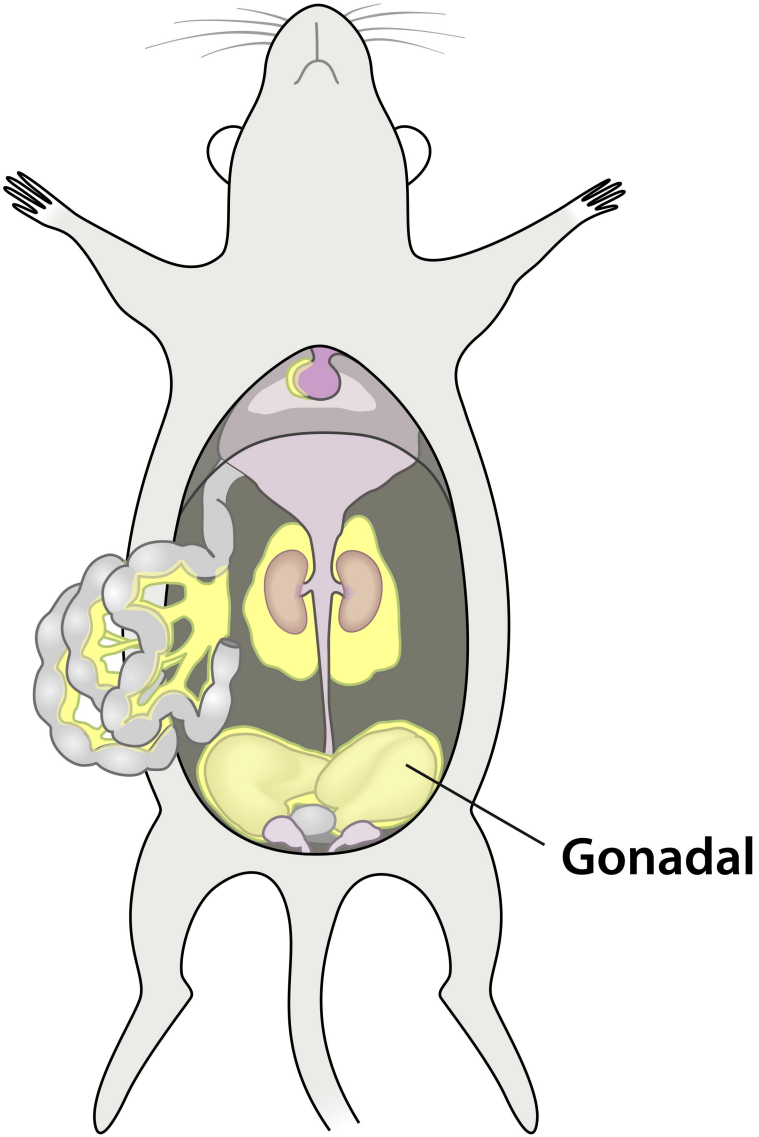
Gonadal

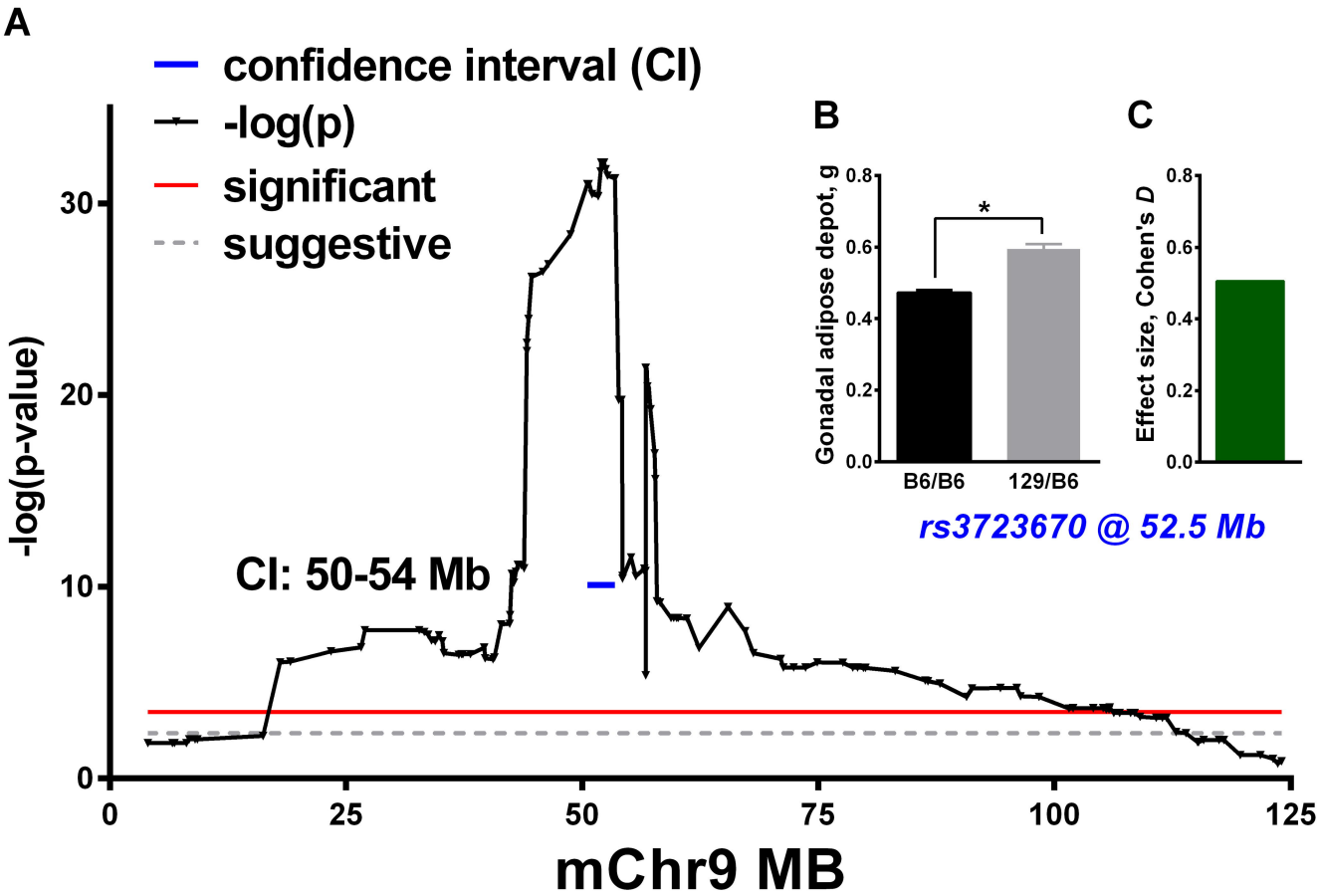
A
confidence interval (CI)
-log(p)
significant
suggestive
-log(p-value)
30
20
10
0
CI: 50-54 Mb
0
25
50
75
100
125
mChr9 MB
B
Gonadal adipose depot, g
0.8
0.6
0.4
0.2
0.0
*
B6/B6
129/B6
C
Effect size, Cohen's D
0.8
0.6
0.4
0.2
0.0
rs3723670 @ 52.5 Mb

A

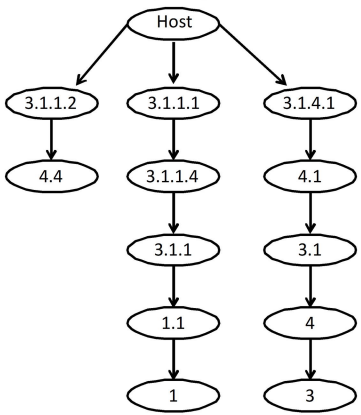

B

Gonadal adipose, g

Strain	Mean	SEM	N	Comparison	*P*-value	Model
Host	0.47	0.00	475			
3.1.4.1	0.50	0.01	13	3.1.4.1 = Host	0.457	
4.1	0.46	0.00	18	4.1 = 3.1.4.1	0.362	
3.1	0.60	0.00	47	3.1 > 4.1	0.000	QTL2+QTL3
4	0.51	0.00	105	4 < 3.1	0.001	QTL1+QTL2+QTL3
3	0.52	0.01	30	3 = 4	0.877	QTL2+QTL3+QTL4
3.1.1.1	0.38	0.00	53	3.1.1.1 < Host	0.000	QTL3
3.1.1.4	0.31	0.01	26	3.1.1.4 = 3.1.1.1	0.068	QTL3
3.1.1	0.52	0.00	34	3.1.1 > 3.1.1.4	0.000	QTL2+QTL3
1.1	0.62	0.00	48	1.1 > 3.1.1	0.003	QTL1+QTL2+QTL3
1	0.57	0.01	19	1 = 1.1	0.195	QTL1+QTL2+QTL3
3.1.1.2	0.39	0.01	15	3.1.1.2 = Host	0.068	
4.4	0.49	0.00	28	4.4 > 3.1.1.2	0.046	QTL1

C

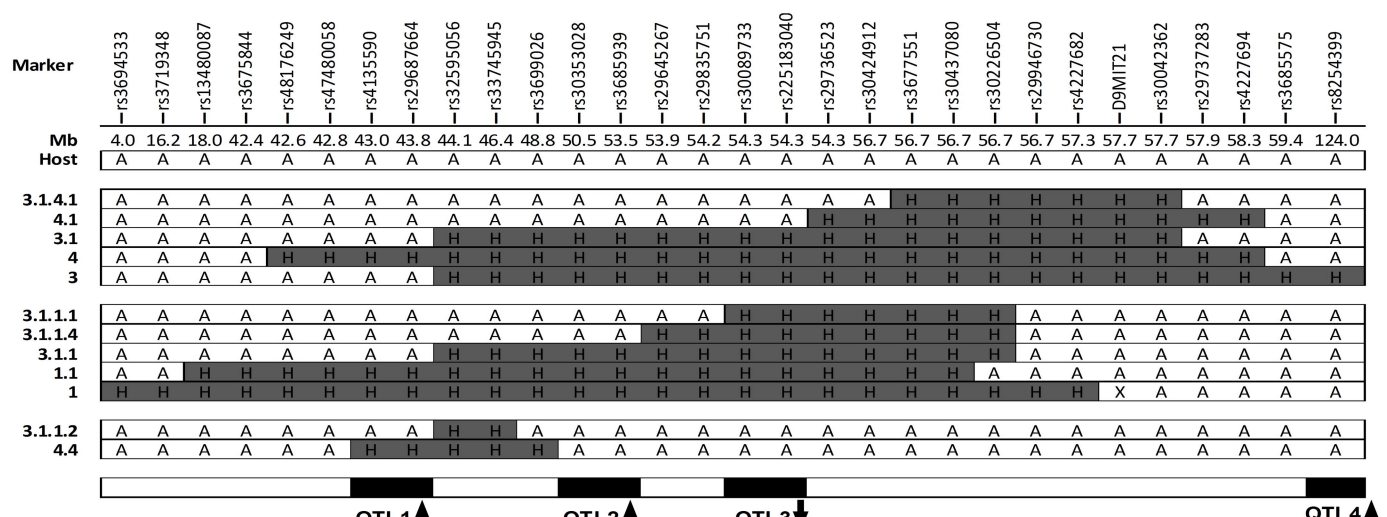

A

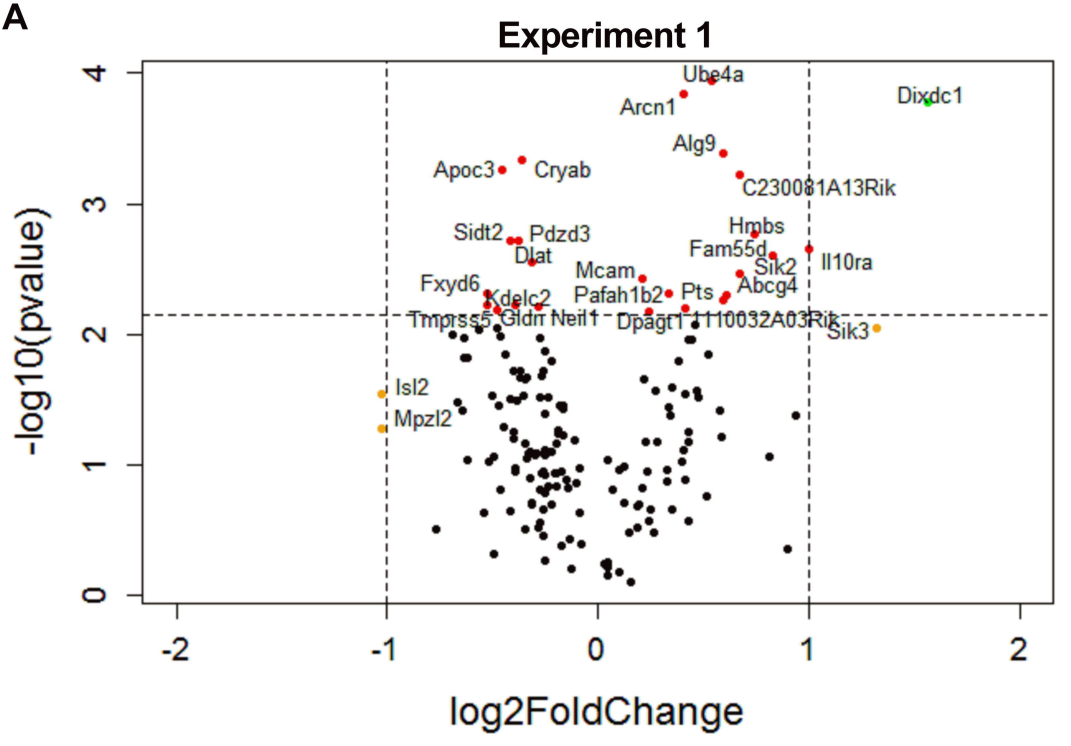
Experiment 1
Ube4a
Arcn1
Dixdc1
Alg9
Apoc3
Cryab
C230081A13Rik
Sidt2
Pdzd3
Hmbs
Fam55d
Dlat
Sik2
Il10ra
Mcam
Fxyd6
Abcg4
Kdelc2
Pafah1b2
Pts
Tmprss5
Gldn
Neil1
Dpagt1
1110032A03Rik
Sik3
Isl2
Mpzl2
-log10(pvalue)
log2FoldChange
-2
-1
0
1
2
0
1
2
3
4

B

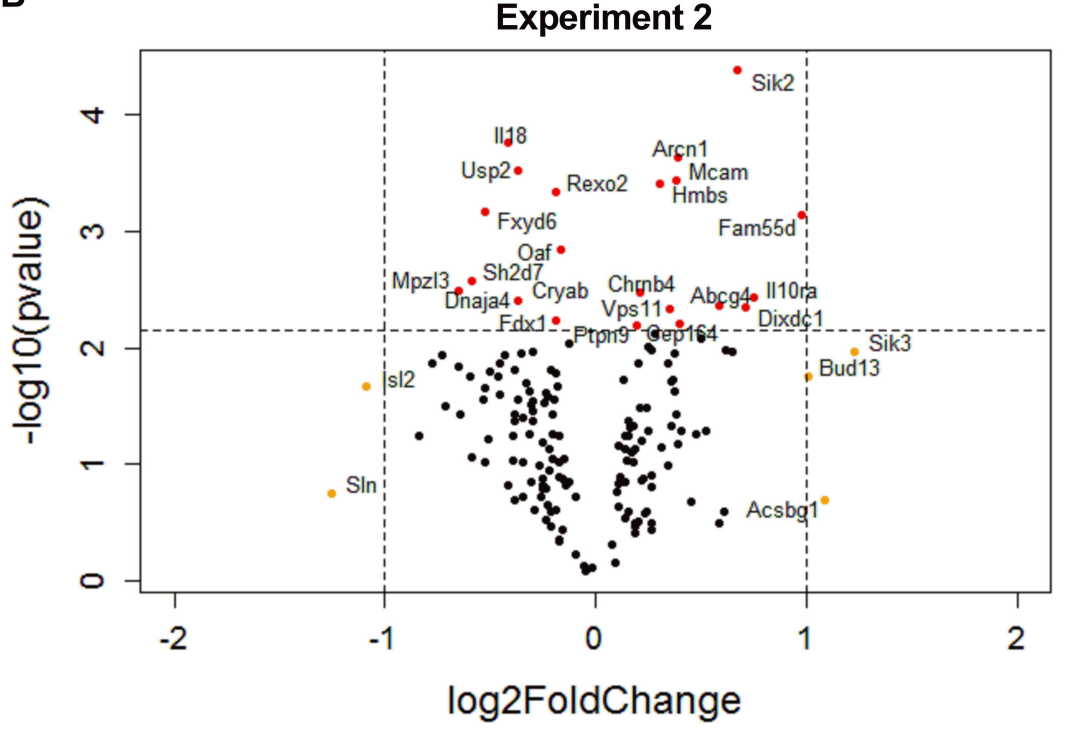
Experiment 2
Sik2
Il18
Arcn1
Usp2
Mcam
Rexo2
Hmbs
Fxyd6
Fam55d
Oaf
Sh2d7
Mpzl3
Cryab
Chrnb4
Abcg4
Il10ra
Dnaja4
Vps11
Dixdc1
Fdx1
Ptpn9
Cep164
Sik3
Bud13
Isl2
Sln
Acsbg1
-log10(pvalue)
log2FoldChange
-2
-1
0
1
2
0
1
2
3
4

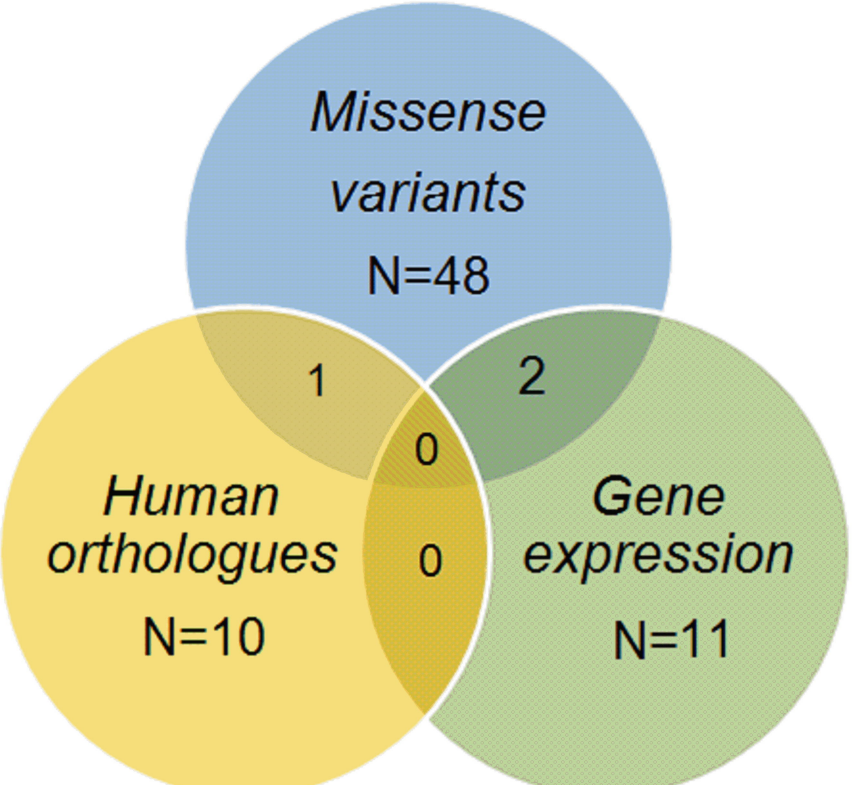
Missense variants
N=48
1
2
0
Human orthologues
N=10
0
Gene expression
N=11